

## Influence of active layer thickness on electrical properties of P3HT/*n*-Si based hybrid heterostructure

Abhiram Gundimeda<sup>a,b</sup>, Monu Mishra<sup>a,b</sup>, Razi Ahmad<sup>a</sup>, Ritu Srivastava<sup>a</sup>, Umesh K Dwivedi<sup>c</sup> & Govind Gupta<sup>a,b\*</sup>

<sup>a</sup>Physics of Energy Harvesting, CSIR-National Physical Laboratory, Dr K S Krishnan Marg, New Delhi 110 060, India

<sup>b</sup>Academy of Scientific and Innovative Research (AcSIR), CSIR-NPL Campus, New Delhi 110 060, India

<sup>c</sup>Amity School of Engineering and Technology, Amity University Rajasthan, Jaipur 303 002, India

*Received 6 October 2016; accepted 26 December 2017*

In the present study, we analyze the effect of active (organic) layer thickness on the optical and electrical properties of poly 3-hexylthiophene/*n*-silicon hybrid hetero-structure. The organic/inorganic sandwiched heterojunction have been prepared via spin-coating of poly 3-hexylthiophene film onto an oxide passivated Si substrate at room temperature. The device structure has been fabricated via depositing silver and aluminum contacts on Poly 3-hexylthiophene and *n*-silicon layers, respectively. The optical and electrical properties of the fabricated heterostructures have been examined by varying the active layer thickness from 50 to 120 nm. Photoluminescence measurements displayed a sharp intense peak at 578 nm corresponding to characteristic poly 3-hexylthiophene band-to-band transition. Enhancement in forward current and reduction in leakage current was observed with increased active layer thickness. It has been observed that employing an active layer thickness of 100 nm, the device produces enhanced forward currents with low leakage currents which leads to the formation of high quality heterojunction and demonstrates better performance of the device.

**Keywords:** Hybrid heterostructure, Poly 3-hexylthiophene, Silicon

### 1 Introduction

A hybrid heterostructure is a unique combination of using good electrical properties of inorganic materials with the film-forming properties of organic polymers. Organic-inorganic heterostructures (OIH) can adapt the merits of inorganic materials<sup>1</sup> (stability, high carrier mobility and absorption up to infrared etc) and exploit the advantages of organic materials (enhanced light absorption, adjustable molecular structures, facile solution processability, high hole mobility etc) for better performance of the device<sup>2</sup>. Fabrication of OIH helps in the development of cost effective flexible electronics, optoelectronics and photovoltaics which offer a new class of semiconductor devices having prospective application in device technology<sup>3</sup>. In recent years, conjugated polymer-inorganic hybrid systems attracted extensive attention<sup>4-13</sup>. Even though the power conversion efficiencies of the OIH remains low, the trend of efficiency increases in these cells is still apparent indicating another exciting prospect to achieve cost effective energy. Of these organic polymers, polythiophenes and their derivatives are an important

class of conjugated polymers for range of optoelectronic applications<sup>14,15</sup>. However, the most important aspect of OIH is the interface formation between the organic and inorganic materials which need to be explored further. The key challenges like optimum thickness of the organic active layer in OIH and the current transport mechanism were important issues which needs to be addressed. A thicker active layer can help to absorb more light, but it may be inefficient for charge transport and collection whereas, very thin layers can hamper the carrier generation and lead to high carrier recombination. Even though exciton diffusion length is shorter in polymers, to absorb sufficient amount of light for efficient photo carrier generation, the thickness of the active layer should be near to the absorption depth of the respective polymers. The main challenge that arises in fabricating the devices based on the OIH is the limitation of interfacial donor-acceptor (DA) area by the surface of the distinct polymer-inorganic interface.

Silicon, due to its high carrier mobility, can be used as an inorganic acceptor. In order to compensate the low charge mobility of the organic materials when compared with inorganic materials, polymer with high absorption coefficient is required to produce more

\*Corresponding author (E-mail: govind@nplindia.org)

charge carriers and increase the device performance. Owing to its high absorption coefficient ( $10^5 \text{ cm}^{-1}$ ) in visible spectra<sup>16</sup> and high charge carrier mobility<sup>17,18</sup> ( $10^{-4} \text{ cm}^2 \text{ V}^{-1} \text{ s}^{-1}$ ), poly (3-hexylthiophene) being a hole conducting polymer, can be used as an organic donor. Highly regio-regular poly 3-hexylthiophene is relatively easy to synthesize and process, relatively stable, making it cost friendly for optoelectronic device applications<sup>19</sup>.

As for the analysis of OIH, extensive research was being carried out in the field of hybrid heterostructures because of its many advantages. Oyama *et al.* investigated a heterojunction of pentacene and *n*-silicon<sup>20</sup>. They examined the diode characteristics to clarify current conduction mechanism at the junction in OIH. In spite of many advantages of hybrid heterostructures, the reported hybrid device performances are still low. The optical absorptivity, which plays a significant role in governing the device performance, greatly depends on the thickness of the hybrid active layer. Even though the poly 3-hexylthiophene /*n*-silicon diode Capacitance-Voltage and Current-Voltage measurements were reported by many groups<sup>21,22</sup>, the substantial effect of active layer thickness on the charge transport phenomenon at organic/inorganic interface was yet to be explored in detail<sup>23</sup>. Xu *et al.* mentioned that the thickness of the layer for bulk heterojunction should be in between<sup>24</sup> 100 to 300 nm, but the study of thickness in bilayer heterostructure is still not premeditated yet. Wang *et al.* investigated the poly 3-hexylthiophene /*n*-silicon hybrid heterostructures via optical simulation using finite difference time domain (FDTD) method to understand the photocurrents in the device but the devices were not fabricated physically<sup>25</sup>.

In this work, we have performed analysis of optical and electrical properties of a bilayer OIH of poly 3-hexylthiophene /*n*-silicon, fabricated via spin coating at varying organic layer thickness. Poly 3-hexylthiophene was used as light absorbing and hole transport layer while silicon was employed as an electron transport layer in the heterostructure. The performance of the heterostructure was systematically investigated under light and dark conditions. The device parameters were calculated, compared and discussed.

## 2 Experimental Procedure

To fabricate poly 3-hexylthiophene /*n*-silicon heterostructure, cleaned silicon (111) samples (*n*-type,

Ph-doped, resistivity 10-20  $\Omega\text{-cm}$ , size  $\sim 8 \times 8 \text{ mm}^2$ ) with a thickness of  $325 \pm 25 \mu\text{m}$  were used. The silicon wafer was chemically pre-cleaned using modified Shiraki process<sup>26</sup>. Subsequently, wafers were etched in 5% HF solution for 5 min in order to eliminate the native oxide and finally rinsed with deionized water for 30 s. The solution of poly 3-hexylthiophene was prepared by taking 10 mg of poly 3-hexylthiophene dissolved in 1 mL 1,2-dichlorobenzene solution. The 50, 80, 100 and 120 ( $\pm 2$ ) nm thin P3HT films were spin coated onto the surface of silicon substrate and dried at room temperature (RT). The metallic contacts were fabricated by thermally evaporating silver and aluminum metals through a shadow mask on the top and bottom of the substrate in the vacuum system operating at a pressure of  $4 \times 10^{-6}$  Torr. The thickness of the silver and aluminum metals was kept to  $\sim 150$  ( $\pm 5$ ) nm each.

The poly 3-hexylthiophene /*n*-silicon (OIH) structures having dimensions of  $0.8 \times 0.8 \text{ cm}^2$  with silver and aluminum contacts were fabricated. The schematics of fabricated P3HT/*n*-silicon heterojunction device was depicted in Fig. 1. The current-voltage (*I-V*) measurement of the device was performed in dark and light ( $100 \text{ mW/cm}^2$ ) conditions with the help of a computer controlled Keithley 2420 source meter. The photoluminescence (PL) spectra of the samples were recorded by light excitation of 450 nm from Fluorolog (JobinYvon Horiba) setup using a Xenon lamp.

## 3 Results and Discussion

The photoluminescence (PL) response of the P3HT/*n*-silicon heterostructure with varying active

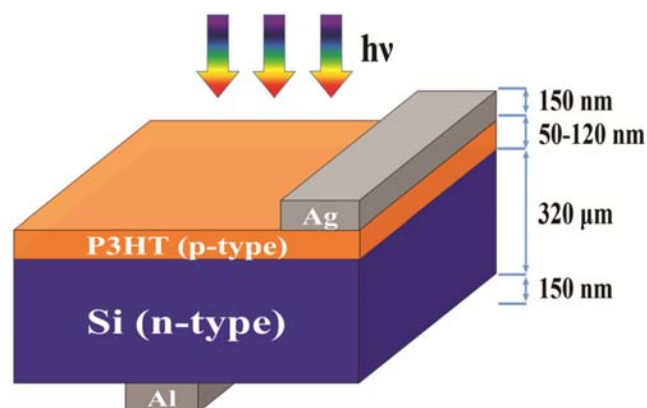


Fig. 1 – Schematics of P3HT/*n*-Si heterostructure with silver (Ag) and aluminum (Al) contacts.

layer thickness is shown in Fig. 2. The OIH displayed an intense peak at 578 nm corresponding to P3HT layer. The shoulder peak around 625 nm was attributed to the  $\pi-\pi^*$  transition associated with P3HT. The intensity of the characteristic peak

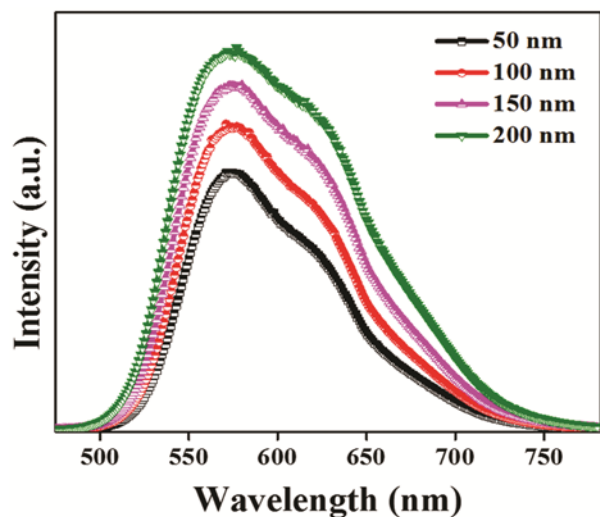


Fig. 2 – Photoluminescence (PL) spectrum of fabricated P3HT/n-Si heterostructure with different active layer thickness.

increased with active layer (P3HT) thickness. No other changes were perceived in PL spectra (except the change in the intensity) with the variation in active layer thickness. The increment in PL intensity can be correlated to the absorption of photons. Due to the high absorption coefficient of P3HT, as the thickness of the active layer increases, it absorbs more photons thereby producing more charge carriers leading to increase in intensity of the PL spectra. The raise in intensity can elucidate that the generation of photo carriers was higher for higher active layer thickness, i.e., at 120 nm.

The current-voltage ( $I$ - $V$ ) characteristics of the fabricated OIH structure (in dark and light conditions) are shown in Fig. 3. At room temperature, the  $V$ - $I$  characteristics of P3HT/ $n$ -silicon heterostructure in the dark condition (Fig. 3(a)) were nonlinear, asymmetric and demonstrated a rectifying behaviour. The leakage currents were small and observed to be in the range of  $\sim 10^{-7}$ -  $10^{-8}$  A. The low value of leakage current indicates that the leakage pathways were short and validates the formation of better P3HT/Si interface. The short leakage pathways specifies that

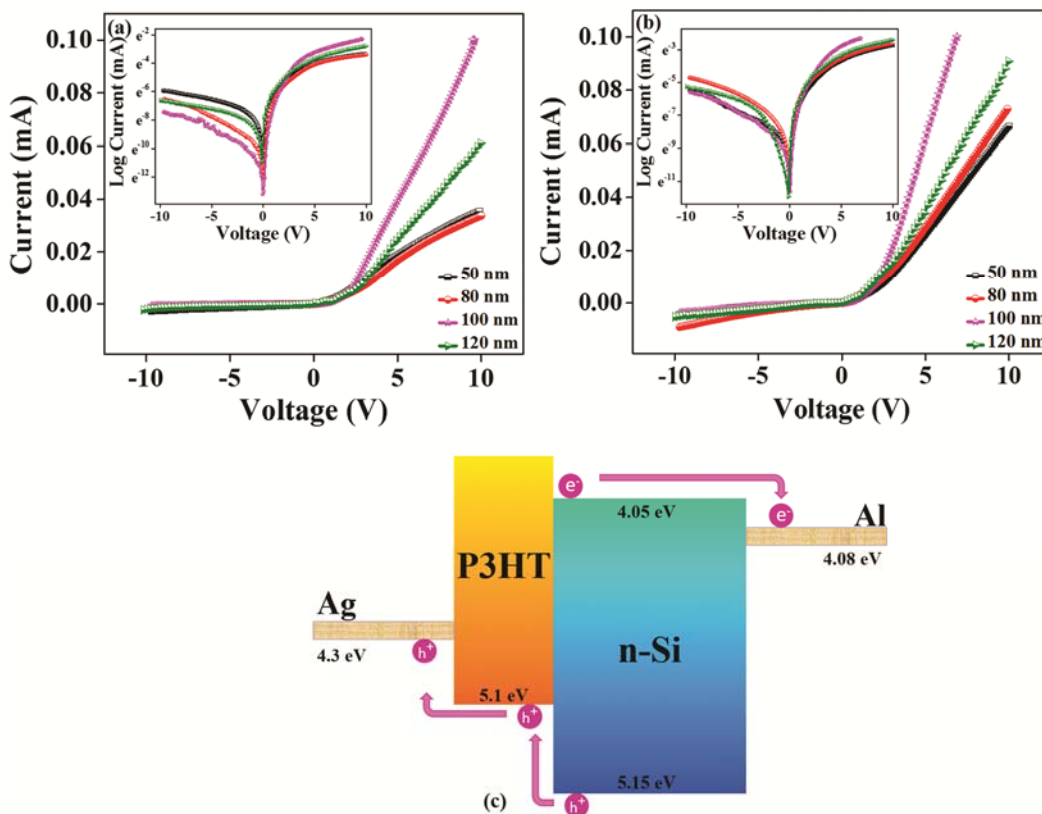


Fig. 3 – (a) Dark and (b) light  $I$ - $V$  characteristics of the device based on P3HT/ $n$ -Si heterostructure at 50 nm, 80 nm, 100 nm and 120 nm thicknesses of the organic P3HT layer.

the recombination of holes and electrons is low, which helps in increasing the effective charge transport of the carriers from the donor region to interface and accept or region to metallic contact. The rectifying behaviour strongly depends on series resistance and interface states. Lower the interface density and the series resistance, greater is the range over which  $I$ - $V$  curve yields a straight line. In the dark  $I$ - $V$  characteristics (Fig. 3(a)), the OIH having organic layer thickness of 100 nm displayed enhanced forward current of 38 mA, followed by 24.9 mA for 120 nm thick active layer. However, a slight difference in forward current between 50 and 80 nm organic layer thicknesses was also observed to be 18.9 mA and 16.2 mA, respectively, where the OIH having active layer thickness of 50 nm displayed slightly higher forward current than organic layer having 80 nm thicknesses.

Under the light conditions (Fig. 3(b)), the OIH with 100 nm thickness produced highest forward current of 62 mA followed by 35, 28.87, 26.11 mA for 120, 80 and 50 nm active layer thicknesses, respectively. We can observe an increase in forward current for 100 nm thick layer was more than two times when compared with 50 nm. This can be attributed to the fact that the effective area of organic layer in which the charge generation, separation and transfer takes place, was increased with thickness. As the photon absorption takes place, the charge carriers were generated in the form of electron-hole ( $E$ - $H$ ) pair in active layer. The pair gets separated near the P3HT/Si interface. The difference in electron affinity of P3HT and Si are enough for producing necessary energy for splitting of the  $E$ - $H$  pair. The holes travel to the anode through P3HT while electrons to the cathode through Si as shown in Fig. 3(c). The increase in effective area (which is due to thickness variation) helps in the generation and transportation of more charge carriers and thereby led to high forward currents. However, the declination in forward current at 120 nm thickness may be ascribed to increased charge carrier recombination at higher thickness. Due to the low exciton diffusion length of the charge carriers in conjugated polymers<sup>27-29</sup>, as the thickness goes beyond 100 nm, the non-radiative recombination may occur and lead to lower availability of charge carriers. Further increasing the active layer thickness beyond 100 nm will also lead to the reduction in absorptivity and enhancement in reflectivity at this wavelength region of 650 nm so thickness of 100 nm

acts as a cut-off thickness after which P3HT starts acting as a non-absorbing dielectric shell which drastically increases the optical absorption in the substrate<sup>25</sup>. So proper choice of organic layer thickness is highly required to enhance light absorption in the device. The reverse bias currents of 100 nm and 80 nm were similar and the decrease was further followed by 120 and 50 nm. So, an organic layer thickness of 100 nm is proposed to be coated onto the surface of silicon substrate to obtain maximum optical absorption. But taking into account the exciton diffusion length (approximately 10 nm), this proposed thickness is much larger. A substantial study was carried out by Paulus *et al.* regarding the exciton diffusion length in which they presented theoretical results supported by the experimental outputs on nano- heterojunction organic solar cells. Here for their device, they proposed that at a P3HT photoactive layer thickness of 60 nm, their devices are producing maximum photocurrents due to bulk exciton sink in P3HT<sup>30,31</sup>. So, by considering that the exciton dissociation mechanism is similar for our P3HT/ Si hybrid heterostructure as proposed by Paulus *et al.*, the active organic P3HT layer thickness can be significantly increased beyond the exciton diffusion length.

The enhancement of the forward current with the active (organic) layer thickness can be explained by the current rectification equation of a Schottky diode<sup>32,33</sup>. The Schottky rectification equation is given as:

$$I = I_s \left[ \exp \left[ \frac{q(V - I R_s)}{nKT} \right] - 1 \right] \quad \dots (1)$$

Where  $q$  is the unit charge,  $n$  is the ideality factor,  $R_s$  is the series resistance at unit area,  $K$  is the Boltzmann constant,  $T$  is the absolute temperature,  $S$  is the device area and  $I_s$  is the saturation current. According to the thermionic emission theory, the saturation current (in relation with Schottky barrier height) is defined by<sup>34</sup>:

$$I_s = SA^{**}T^2 \exp \left( - \frac{q\phi_B}{KT} \right) \quad \dots (2)$$

Where  $\phi_B$  is the Schottky barrier height,  $A^{**}$  is the Richardson constant and equals to:

$$A^{**} = \frac{4\pi m K^2 q}{h^3} \quad \dots (3)$$

In case of Si,  $A^{**}$  equals to 110 A/cm<sup>2</sup>K<sup>235</sup>.

The slope of the linear region of the forward bias in  $I$ - $V$  curve gives us the ideality factor ( $n$ ) by using the relation:

$$n = \frac{q}{KT} \frac{dV}{(\ln I)} \quad \dots (4)$$

We can clearly witness the shift in output current with increasing thickness of the active layer, which is due to increase in effective resistance of the structure. With an increase in thickness of P3HT layer, there is a gradual increase in the output current. The reverse saturation current was obtained to be  $3.5E-7$ ,  $5.9E-8$ ,  $2E-8$  and  $1.7 E-7A$  (under a bias of 5 V) for organic layer thickness of 50, 80, 100 and 120 nm, respectively. The OIH revealed lowest reverse saturation current at 100 nm because the drift of minority carriers (i.e., electrons from  $p$ -type and holes from  $n$ -type) towards the depletion region is low at this thickness. It is well known that the dark current in a diode is dominated by majority carrier injection (electron injection in  $n$ -type Si) into the metal anode. So, the reduction in dark current is an evidence of reduced electron current. At 120 nm, the reduced forward current under dark condition is due to the high carrier recombination at the heterojunction as well as the increase in series resistance of the device.

Figure 4 shows the organic layer thickness versus rectification ratio (Fig. 4(a)) and barrier height (Fig. 4(b)). The rectification ratio (RR) is the ratio of forward current to the reverse current at a particular voltage. The RR values (at  $\pm 5$  V) were calculated to be  $12.6 \pm 0.63$ ,  $46.38 \pm 2.31$ ,  $508.33 \pm 25.4$  and  $69.16 \pm 3.46$  for the thickness of 50, 80, 100 and 120 nm, respectively. The high RR value obtained for 100 nm indicates efficient charge injection through the polymer under forward bias, and much less so under reverse bias, thereby forming high quality interface in OIH. A high RR value can be attributed to two factors: one is that the silicon and P3HT are displaying better transport properties with increasing

thickness, consisting of high electron mobility<sup>36</sup> and hole mobility<sup>37</sup> to provide the charge carriers with a direct electrical pathway<sup>38-40</sup> and other factor is the formation of high quality P3HT/ $n$ -silicon interface in the device.

The values of the ideality factor ( $n$ ) were obtained by using Eq. (4) and calculated to be 1.84, 1.81, 1.47 and 1.69 ( $\pm 0.05$ ). The obtained  $n$  values are higher than unity. The presence of the ideality factor more than unity indicates the generation of an interfacial layer and interface states at the heterojunction. It is also ascribed to the high value of series resistance ( $R_s$ ) and interface states. It is associated with a relatively large voltage drops at the interface. The deviation of  $n$  from unity corresponds to recombination of electrons and holes near the depletion region, and the increase of the diffusion current due to increasing applied voltage. It is evaluated that if  $n$  value is 1, then the device is governed by diffusion currents, but the  $n$  value greater than 2 corresponds to the dominance of recombination current. The obtained  $n$  value confirms the presence of both recombination and diffusion currents in OIH. The ideality factor decreased with increasing organic layer thickness. At 100 nm, the device ideality factor is closer to unity (ideal diode) which shows that OIH fabricated at 100 nm is better among all the fabricated devices.

Figure 4(b) represents the potential barrier height values with varying thickness of the organic layer. The barrier heights were calculated by using Eq. (2) and were found to be 0.82, 0.84, 0.78 and 0.82 eV ( $\pm 2$  meV) for layer thickness of 50, 80, 100 and 120 nm, respectively. The increase in barrier height of the OIH is due to the interface between metal/semiconductor passivated by P3HT organic layer surface. The deposition of P3HT on  $n$ -silicon, lead to the

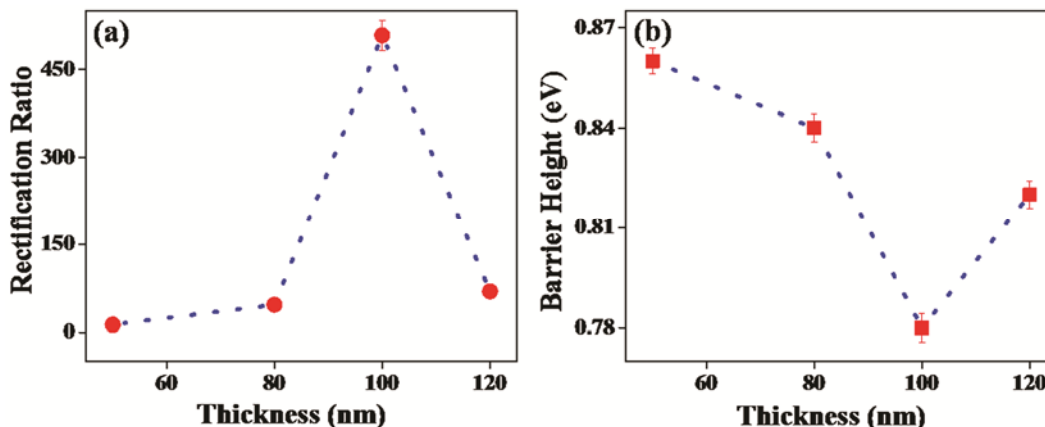


Fig. 4 – (a) Organic layer thickness versus rectification ratio and (b) organic layer thickness versus voltage barrier height.

Table 1 – Variation of series and shunt resistance with organic layer thicknesses.

Thickness (±2) (nm)	Series resistance (±8) (Ω)	Shunt resistance (±0.03) (kΩ)
50	893	2.37
80	883	4.92
100	492	6.69
120	737	7.25

realignment of the highest occupied molecular orbital and lowest unoccupied molecular orbital levels of the organic semiconductor with the metal work function, which affected the surface interaction. It leads to the change in the electron affinity of the semiconductor at the organic/inorganic interface and results an increase in the barrier height.

In the organic donor polymers, non-radiative decays will occur when excitons are bound towards cathode, causing imbalance in charge carriers in the donor layer. The imbalance in the charge carriers directly affects the interface in OIH, as with increase in the organic layer thickness the exciton generation will be higher. So, due to high exciton generation, more charge carriers move towards the barrier leading to increased non-radiative recombination. Due to weak Vanderwaal intermolecular bonding, organic interfaces are formed with weakly interacting boundaries and also due to active defects. It leads to formation of interface with gap states. So increase in thickness facilitates more gap states thereby resulting in high recombination. Hence, this imbalance in the number of charge carriers and the presence of defect states, variation in mobile charge carriers in the donor leads to shift in the barrier height.

It was observed that at higher voltage in forward bias, the junction resistance approaches a constant value, which is considered as series resistance ( $R_s$ ) while in reverse bias the maximum value of junction resistance is equal to diode shunt resistance ( $R_{sh}$ ). In general,  $R_{sh}$  arises from charge recombination at the donor/acceptor (D/A) interface and surface current leakage while  $R_s$  is affected by the bulk resistance of the active layer and the contact resistance between the active layer and the electrode. The values of series and shunt resistances of the fabricated P3HT/*n*-silicon devices are tabulated in Table 1. The  $R_s$  of the OIH was perceived to be minimal for the organic layer thickness of 50 nm. For same value of current, the rise in series resistance results in increase of the voltage drop between the junction voltage and the terminal voltage. In order to compensate this drop, reduction of

the terminal voltage takes place. The shunt resistance values should be as high as possible for high terminal current. In this case,  $R_{sh}$  is high for the active layer thickness of 120 nm highlighting the increase in shunt resistance with increasing thickness. However the values of the  $R_s$  and  $R_{sh}$  that we obtained lead to a conclusion that at active layer thickness of 100 nm, the device shows enhanced performance which is in agreement with the *I-V* characteristics.

#### 4 Conclusions

In summary, OIH of P3HT/*n*-silicon were fabricated via spin-coating the P3HT layer with a thickness varying from 50-120 nm. The fabricated P3HT/*n*-silicon hybrid heterojunction displayed sharp rectifying properties. The forward current in dark as well as light condition was highest for OIH having organic layer thickness of 100 nm. The rectification ratio varied from 12-508 at ±5 V and revealed highest value (i.e., 508) for 100 nm thickness of active layer. The device with 100 nm active layer thickness yielded lowest reverse saturation current with ideality factor of 1.47, which indicates the formation of high quality interface and better charge generation and transport in the device. Variation of series and shunt resistance with layer thickness was also analyzed which lied in intermediate regime for 100 nm thick OIH. It can be concluded that OIH having organic layer thickness of 100 nm forms better interface thereby producing efficient device.

#### Acknowledgement

The authors would like to acknowledge the Director, CSIR-NPL, New Delhi, for his constant encouragement and support. This work is financially supported by CSIR project TAPSUN (NWP-55) and Department of Science & Technology, GoI under grant aid DST-GAP-160732.

#### References

- Gunes S & Sariciftci N S, *Inorg Chim Acta*, 361 (2008) 581.
- Helgesen M, Sondergaard R & Krebs F C, *J Mater Chem*, 20 (2010) 36.
- Chandrasekaran J, Nithyaprakash D, Ajjan K B, Maruthamuthu S, Manoharan D & Kumar S, *Renew Sust Energ Rev*, 15 (2011) 1228.
- Roland S, Neubert S, Albrecht S, Stannowski B, Seger M, Facchetti A, Schlattmann R, Rech B & Neher D, *Adv Mater*, 27 (2015) 1262.
- Ghadirzadeh A, Passoni L, Grancini G, Terraneo G, Bassi A L, Petrozza A & Fonzo F D, *ACS Appl Mater Interfaces*, 7 (2015) 7451.

- 6 Xu Q, Song T, Cui W, Liu Y, Xu W, Lee S T & Sun B, *ACS Appl Mater Interfaces*, 7 (2015) 3272.
- 7 Mac L J, Rath T, Cappel U B, Dowland S A, Amenitsch H, Knall A C, Buchmaier C, Trimmel G, Nelson J & Haque S A, *Adv Funct Mater*, 25 (2015) 409.
- 8 Kus M, Ozel F, Buyukcelebi S, Aljabour A, Erdogan A, Ersoz M & Sariciftci N S, *Opt Mater*, 39 (2015) 103.
- 9 Radychev N, Kempken B, Krause C, Li J, Olesiak J K, Borchert H & Parisi J, *Org Elec*, 21 (2015) 92.
- 10 Ishii A & Hasegawa M, *Sci Rep*, 5 (2015) 11714.
- 11 Chehata N, Ltaief A, Ilahi B, Salam B, Bouazizi A, Maaref H & Beyou E, *Syn Mater*, 191 (2014) 6.
- 12 Ding Y, Gresback R, Liu Q, Zhou S, Pi X & Nozakl T, *Nan Energy*, 9 (2014) 25.
- 13 Duché D, Bencheikh F, Dkhil S B, Gaceur M, Berton N, Margeat O, Ackermann J, Simon J J & Escoubas L, *Sol Energy Mater Solar Cells*, 126 (2014) 197.
- 14 Kim Y, Cook S, Tuladhar S M, Choulis S A, Nelson J, Durant J R, Bradley D D C, Giles M, McCulloch I, Ha C S & Ree M, *Nat Mater*, 5 (2006) 197.
- 15 Liang Y, Xu Z, Xia J, Tsai S T, Wu Y, Li G, Ray C & Yu L, *Adv Mater*, 22 (2010) E135.
- 16 Deibel C & Dyakonov V, *Rep Prog Phys*, 73 (2010) 096401.
- 17 Ballantyne A M, Wilson J S, Jenny N, Bradley D D C, Durrant J R, Heeney M, Duffy W & McCulloch I, *Proc SPIE*, 6334 (2006) 633408.
- 18 Sirringhaus H, Tessler N & Friend R H, *Science*, 280 (1998) 1741.
- 19 Dang M T, Hirsch L & Wantz G, *Adv Mater*, 23 (2011) 3597.
- 20 Oyama N, Takanashi Y, Kaneko S, Momiyama K, Suzuki K & Hirose F, *Microelectron Eng*, 88 (2011) 2959.
- 21 Brus V V, Zellmeier M, Zhang X, Greil S M, Gluba M, Töflinger A J, Rappich J & Nickel N H, *Organic Elec*, 14 (2013) 3109.
- 22 Liu C Y, Holman Z C & Kortshagen U R, *Adv Funct Mater*, 20 (2010) 2157.
- 23 Oyama N, Kaneko S, Momiyama K & Hirose F, *IEICE Trans Elec*, E94 (2011) 1838.
- 24 Xu T & Qiao Q, *Energy Environ Sci*, 4 (2011) 2700.
- 25 Wang W, Li X, Wen L, Zhao Y, Duan H, Zhou B, Shi T, Zeng X, Li N & Wang Y, *Nanoscale Res Lett*, 9 (2014) 238.
- 26 Enta Y, Suzuki S, Kono S & Sakamoto T, *Phys Rev B*, 39 (1989) 5524.
- 27 Halls J J M, Pichler K, Friend R H, Moratti S C & Holmes A B, *Appl Phys Lett*, 68 (1996) 3120.
- 28 Scully S R & McGehee M D, *J Appl Phys*, 100 (2006) 0349070.
- 29 Shaw P E, Ruseckas A & Samuel I D W, *Adv Mater*, 20 (2008) 3516.
- 30 Paulus G L C, Ham M H & Strano M S, *Nanotech*, 23 (2012) 095402.
- 31 Ham M H, Paulus G L C, Lee C Y, Song C, Kalantar-Zadeh K, Choi W, Han J H & Strano M S, *ACS Nano*, 10 (2010) 6251.
- 32 Cheung S K & Cheung N W, *Appl Phys Lett*, 49 (1986) 85.
- 33 Sze S M, *Physics of semiconductor devices*, 2<sup>nd</sup> Edn, (Wiley: New York), 1981.
- 34 Mishra M, Gundimeda A, Krishna S, Aggarwal N, Gahtori B, Dilawar N, Aggarwal V V, Singh M, Rakshit R & Gupta G, *Phys Chem Chem Phys*, 19 (2017) 8787.
- 35 Schwartz G C & Srikrishnan K V, 2<sup>nd</sup> Edn, *Handbook of semiconductor interconnection technology*, (Taylor & Francis), 2006.
- 36 Roest L, Kelly J J & Vanmaekelbergh D, *Phys Rev Lett*, 89 (2002) 036801.
- 37 Morse G E & Bender T P, *ACS Appl Mater Interfaces*, 4 (2012) 5055.
- 38 Olson D C, Lee Y J, White M S, Kopidakis N, Shaheen S E, Ginley D S, Voigt J A & Hsu J W P, *J Phys Chem C*, 111 (2007) 16640.
- 39 Leschkies K S, Divakar R, Basu J, Enache-Pommer E, Boercker J E, Carter C B, Kortshagen U R, Norris D J & Aydil E S, *Nano Lett*, 7 (2007) 1793.
- 40 Takanezawa K, Hirota K, Wei Q S, Tajima K & Hashimoto K, *J Phys Chem C*, 111 (2007) 7218.